JOURNAL OF MATERIALS SCIENCE 21 (1986) 3125–3134

The coking kinetics of heat resistant austenitic steels in hydrogen–propylene atmospheres

P. R. S. JACKSON, D. L. TRIMM, D. J. YOUNG
School of Chemical Engineering and Industrial Chemistry, The University of New South Wales, PO Box 1, Kensington, New South Wales 2033, Australia

The kinetics of coke formation on several commercial Fe–Ni–Cr alloys used in the construction of ethylene steam crackers, nickel and copper were investigated over the temperature range 450 to 1000° C in hydrogen–propylene atmospheres using a tubular microbalance reactor. Between 900 and 1000° C steady state coking was controlled by gas-phase pyrolysis and similar coking rates were observed for all materials. At 900° C alloy carburization led to lengthy periods of parabolic kinetics before the onset of steady state. Below 900° C alloy coking rates were between those of copper and nickel. Major differences in coking rates of alloys were only observed below 800° C and arise from variations in the effectiveness of chromium carbide scales in excluding the hydrocarbon atmosphere from contact with the underlying nickel-rich and iron-rich alloy.

1. Introduction

Heat resistant Fe–Ni–Cr alloys are used as construction materials for steam cracking reactors which produce light olefins from hydrocarbon feedstocks. Build-up of carbonaceous deposits on the inner walls of radiantly heated alloy reactor tubes at temperatures in the vicinity of 900 to 1000° C leads to poor heat transfer and loss of process efficiency. Apart from the regular shutdown and decoking operations which are required as a result, the formation of coke leads to localized overheating, carburization and ultimately reactor tube failure.

The carburization behaviour of heat resistant alloys has been studied over a wide range of varying carbon and oxygen activities [1–8]; however, relatively few studies [9, 10] have been conducted on the coking behaviour of alloys at temperatures appropriate to steam cracking.

Coke formation kinetics on metals such as nickel, which are used as catalysts in hydrocarbon conversion processes at temperatures usually well below 800° C have been reviewed in detail [11, 12]. This work has shown that metallic particles are incorporated into the coke. It has also been found that coke removed from ethylene production plants can contain significant quantities of particulate metals [10, 13] and it is generally considered that metal particles within a coke deposit can catalyse its further growth. The aim of this investigation was to study the coking behaviour of several commercial alloys and to determine whether alloy composition had any effect on the overall rate of coke formation in hydrogen–propylene atmospheres. In addition, the coking behaviour of the alloys was compared with that of nickel, which catalyses the coking reaction, and copper, which is known ([14] p. 109) to be catalytically inactive to coking.

2. Experimental procedures

Kinetics of coke deposition from hydrogen–propylene gas mixtures on metals and alloys were monitored continuously using an electronic (C. I. Electronics Mk. IIB Microforce) microbalance. The experimental arrangement is shown schematically in Fig. 1. Propylene and high purity hydrogen gases were dried using magnesium perchlorate columns and their flow rates monitored with calibrated flow meters. A total gas flow rate of 630 ml min^{-1} at room temperature and 1 atm pressure, corresponding to an inlet residence time of approximately 7 sec, was used in all experiments. A hydrogen flow rate of 57 ml min^{-1} continuously purged the microbalance before entering the reactor whilst propylene and the remaining hydrogen were fed into the reactor directly. Temperature was controlled to $\pm 2°$ C with an electric furnace which was raised or lowered over the reactor at the beginning and end of a run.

The compositions and designations of the alloys used in these experiments are listed in Table I. In addition, nickel (99.9%) and copper (99.95%) were used. Samples were cut to the approximate dimensions 7 mm × 7 mm × 1 mm using a carborundum wheel, abraded to a 400 grit finish on silicon carbide papers, their geometric surface areas measured and then ultrasonically degreased in chloroform. A freshly prepared sample was suspended from the balance beam into the reactor by means of a quartz cradle and fibre. This enabled a constant sample position to be maintained within the hot zone during all experiments. The microbalance reactor assembly was then evacuated and backfilled with hydrogen several times before the introduction of propylene. The gas mixture was passed over the sample for 30 min whilst at room temperature before lifting the preheated furnace over

0022–2461/86 $03.00 + .12

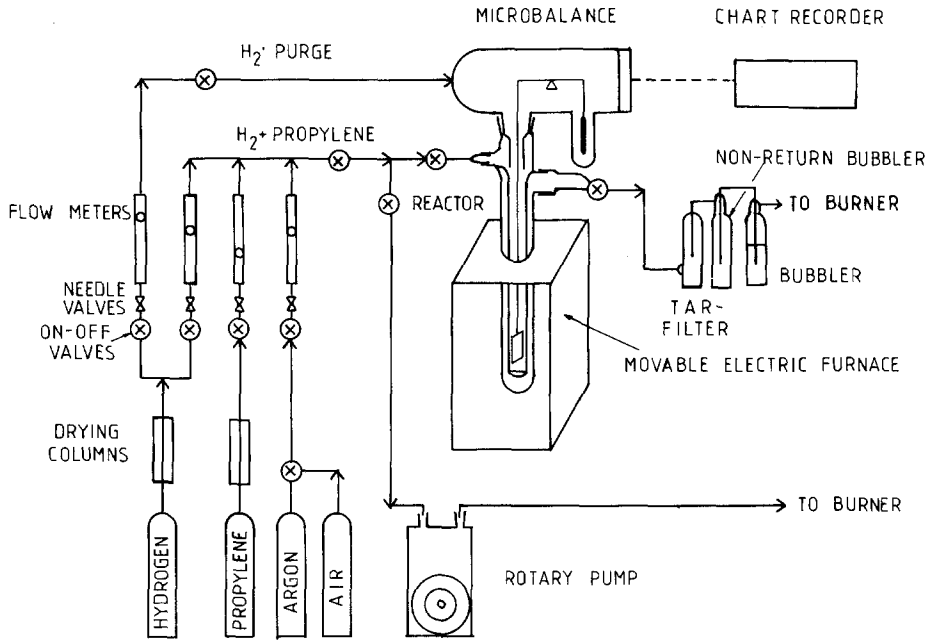

Figure 1 Schematic diagram of experimental apparatus.

the reactor. Hydrogen–propylene molar ratios in these mixtures were varied between 3 : 1 and 62 : 1. The sample reached the required temperature in 10 to 15 min. At the end of a run the furnace was lowered and the sample allowed to cool in the flowing gas before removal for subsequent examination.

In situ X-ray diffraction (XRD), scanning electron microscopy (SEM), energy dispersive analysis of X-rays (EDAX), and stereomicroscopy were used to examine surfaces whilst optical metallography was used to examine polished sample cross-sections.

3. Results

At most temperatures between 450 and 1000° C, steady state linear coking kinetics were observed for all materials in atmospheres containing 3 : 1 molar ratios of hydrogen to propylene as soon as the reactor and specimen reached temperature. Approximately 1 to 2 h, however, were required before the onset of steady state linear coking for nickel at 800° C and for nickel and the alloys at 900° C. During this period reaction rates decreased progressively with time.

At 900° C in atmospheres having 50 : 1 molar ratios of hydrogen to propylene, steady state linear kinetics were never observed, and reaction rates also progressively decreased with time. To illustrate the types of kinetic behaviour which were observed under various conditions, a selection of typical kinetic curves is shown in Fig. 2.

TABLE I Compositions of Fe–Ni–Cr alloys used in coking studies

Alloy	Alloying element (wt %)								
	Fe	Ni	Cr	C	Nb	W	Si	Mn	Other
36XT	13.8	44.8	35.5	0.35	1.34	1.70	1.6	0.9	–
36XS	34.1	34.1	25.9	0.43	1.11	1.52	1.6	1.2	–
2535Nb	34.6	35.2	25.0	0.45	1.57	–	2.2	1.0	–
800H	44.1	32	21	–	–	–	1	1.5	0.4 Ti
HK40	50.7	21.6	24.5	0.4	–	–	1.3	0.6	0.8 Mo

For the time periods where decreasing reaction rates were observed, the kinetics could be described with a parabolic rate equation:

$$\Delta W/A + W' = (k_p t)^{1/2}$$

where $\Delta W/A$ is the weight gain per unit area formed in time, t; k_p is the parabolic rate constant and W' is a constant. These constants were estimated by regression of the data on the above equation.

3.1. Hydrogen–propylene molar ratio of 3 : 1

Coking kinetics at 900° C during the initial period of non-linear reaction are shown in Fig. 3 and the parabolic rate constants observed, are presented in Table II. Steady state linear coking rates (k_l) obtained from the slopes of the linear sections of weight gain–time curves (not shown) for all materials at temperatures between 700 and 1000° C in 3 : 1 hydrogen–propylene atmospheres are presented in Table III.

Fig. 4 shows an Arrhenius plot for the steady state linear rate constant obtained in 3 : 1 hydrogen–propylene atmospheres. For nickel, the Arrhenius plot consists of three regions: a low temperature region ($T \leqslant 550°$ C) with a measured activation energy of $210 \pm 20\,\mathrm{kJ\,mol^{-1}}$; a high temperature region ($T \geqslant 900°$ C) with an activation energy of $243 \pm 8\,\mathrm{kJ\,mol^{-1}}$, and an intermediate temperature region ($550 \leqslant T \leqslant 900°$ C) with a measured apparent activation energy of $-140 \pm 21\,\mathrm{kJ\,mol^{-1}}$. Coke morphologies on nickel changed from filamentous at low and intermediate temperatures to compact layers at 900 and 1000° C (Fig. 5). At 900° C some coke filaments grew above the compact layer (Fig. 5b). The compact deposit was identified by XRD as being graphitic.

In contrast, the rate of coke formation on copper decreased with decreasing temperature and filamentous coke was never observed. Steady state coking rates at 900 and 1000° C were, within experimental reproducibility, identical to nickel. At 700° C, however,

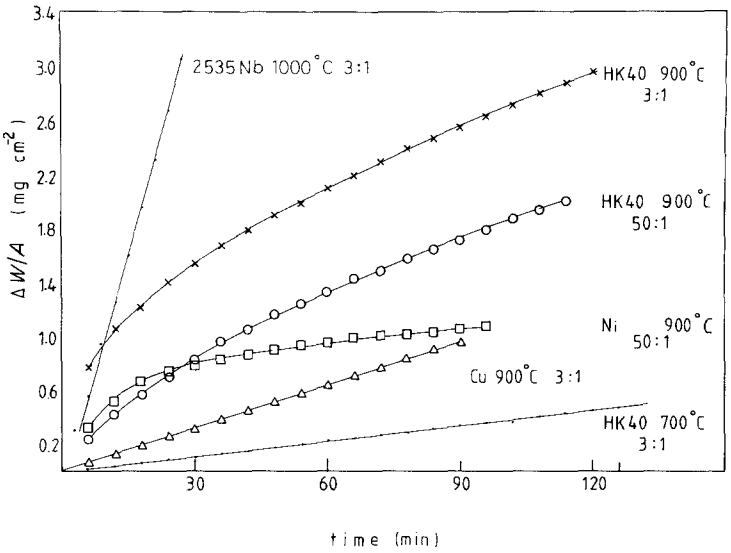

Figure 2 Typical weight uptake kinetics in hydrogen–propylene atmospheres under various experimental conditions.

coking rates on copper were three orders of magnitude lower than on nickel.

Coking rates of the alloys at 700° C varied consideraby and the deposits consisted of localized bundles of interwoven coke filaments. The spatial density and volume of these filamentous coke deposits varied considerably and accounted for the differences in observed rates. For HK40 similar morphologies were observed at temperatures below 700° C and the amount of coke decreased with decreasing temperature (Fig. 5d). At 800° C the alloys had similar coking rates and only minor variations in morphologies were observed. Between 900 and 1000° C the alloys, nickel and copper, all behaved essentially in the same way, having similar coking rates and deposit morphologies consisting essentially of compact graphitic layers.

3.2. Molar ratios of hydrogen to propylene greater than 3:1

Changes in the morphology of coke deposits formed on nickel at 900° C were induced by varying the ratio of hydrogen to propylene in the inlet gas mixture from 3:1 to 62:1. Although less coke was formed at high gas ratios due to a reduction in the volumetric flow rate of propylene, the relative proportion of filamentous to compact coke increased significantly. At hydrogen–propylene ratios greater than approximately 20:1 only filamentous coke was formed.

With the exception of copper, kinetics followed parabolic rather than linear rate laws in 50:1 hydrogen–propylene atmospheres at 900° C. Weight gains for nickel and the alloys are shown in Fig. 6 as a function of $t^{1/2}$ and the parabolic rate constants obtained thereby are shown in Table IV. Coke morphologies consisted of localized bundles of filaments (Fig. 7) which in the case of alloys often formed preferentially around interdendritic areas (Fig. 7c). Back-scattered electron images of the deposits revealed the presence of active catalytic particles at the tips of filaments; however, their number was relatively few and as a result, their composition could not be determined.

An HK40 specimen was reacted for 4 days to obtain sufficient coke for analysis of its metal content. Parabolic reaction kinetics were recorded for 36 h (Fig. 8) and a final weight gain of 16 mg was observed. Almost no coke formed and the alloy was through carburized (Fig. 9).

3.3 Reaction products

Analysis of coked alloys by XRD indicated the presence of graphite having an (0 0 2) lattice spacing of 0.338 nm and an apparent crystallite size of about 20 nm, and the carbides Cr_3C_2 and Cr_7C_3 on the alloy surfaces. In all cases, intense alloy austenite peaks were also observed. The results are summarized in Table V. Formation of Cr_3C_2 was favoured for the low iron alloys, namely 36XT and 36XS, whereas for HK40 and 800H only Cr_7C_3 was detected. Carbides formed at 900 and 1000° C appeared metallographically as very thin external layers and as blocky precipitates within the alloy arising from carburization (Fig. 10). Below 900° C, EDAX analyses of non-coked areas showed enrichment of the surface in both iron and chromium; however, external carbide scales could not be seen. Alloy carburization was not evident below 800° C.

4. Discussion

It has been shown previously [15] that modification of the surface chemistry of an alloy can drastically alter its coking kinetics. The experimental procedure used in this investigation was chosen to prevent possible surface modification prior to an experiment. By not "reducing" the alloy surface in hydrogen prior to coking, the possibilities of chromium loss by evaporation at high temperatures or its oxidation

TABLE II Parabolic rate constants ($mg^2 cm^{-4} min^{-1}$) in 3:1 hydrogen–propylene atmospheres at 900° C

Material	36XT	36XS	2535Nb	800H	HK40	Ni
k_p	9.5×10^{-3}	2.6×10^{-2}	2.1×10^{-2}	–	6.4×10^{-2}	8.6×10^{-2}

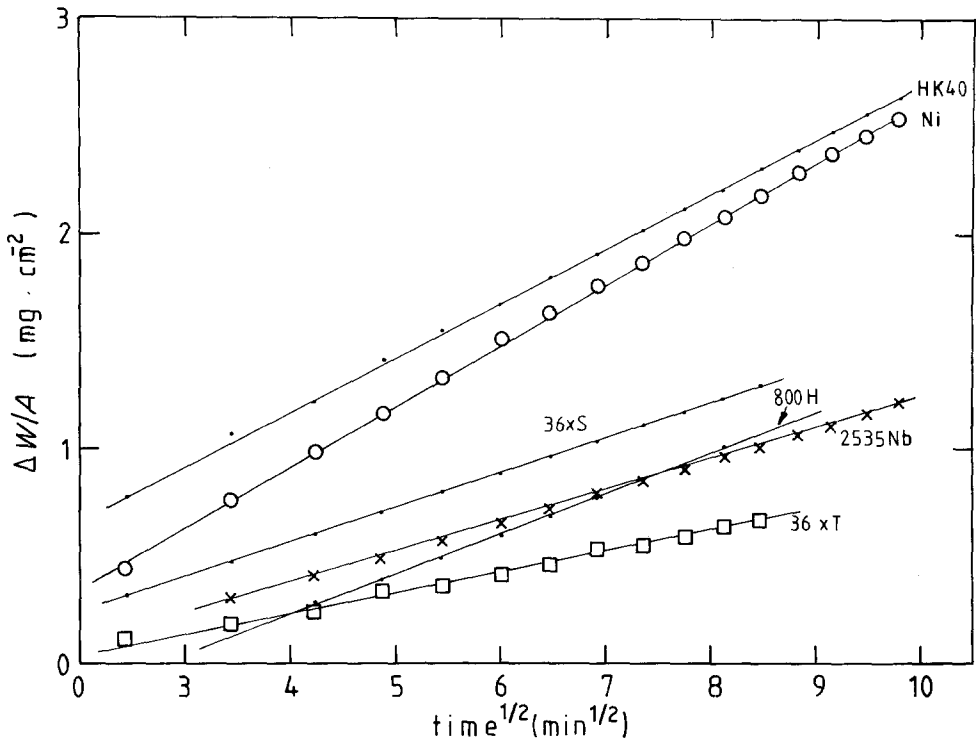

Figure 3 Parabolic plot of initial reaction kinetics at 900° C in 3 : 1 hydrogen–propylene atmospheres.

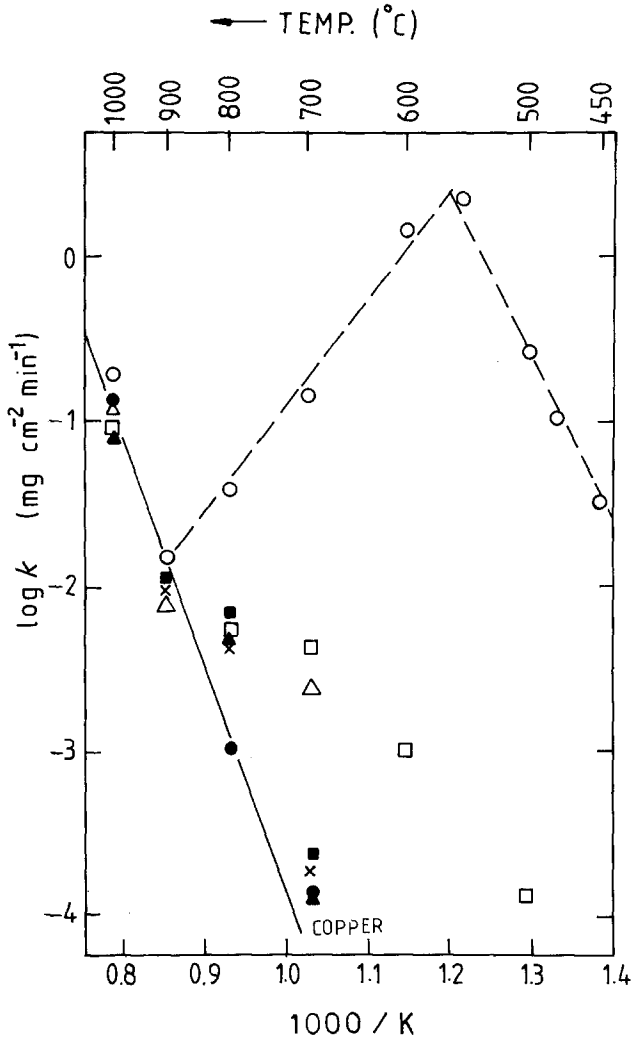

Figure 4 Arrhenius plot of steady state linear coking rates in 3 : 1 hydrogen–propylene atmospheres. ○ Nickel, ● copper, × 36XT, ■ 36XS, △ 2535 Nb, ▲ 800H, □ HK40.

at low temperatures due to trace gas impurities were eliminated.

It is known that coking kinetics are influenced by numerous other variables including gas composition, residence time, reactor design and construction materials upstream, surface roughness, concentration of gaseous species and temperature. The effects of all of these are difficult if not impossible to establish simultaneously and hence coking behaviour of nickel and copper, materials whose behaviour is relatively well understood, was determined for the purpose of comparison

4.1. Coke formation at hydrogen–propylene ratios of 3 : 1

Temperature-dependent steady state coking behaviour observed for nickel was similar to that usually observed for iron and nickel ([15] p. 89) and catalytic metals generally. The low temperature behaviour of the Arrhenius plot (Fig. 5) has been attributed to formation of filamentous coke, where the rate-controlling step is considered to be carbon diffusion through catalytic nickel particles at the heads of growing filaments. Several postulates have been made to account for the driving force for carbon diffusion

TABLE III Steady state linear rate constants ($mg\,cm^{-2}\,min^{-1}$) of materials coked in 3 : 1 hydrogen–propylene atmospheres

	700° C	800° C	900° C	1000° C
Copper	1.3×10^{-4}	1.0×10^{-3}	1.1×10^{-2}	1.3×10^{-1}
Nickel	1.4×10^{-1}	3.8×10^{-2}	1.4×10^{-2}	1.9×10^{-1}
36XT	1.8×10^{-4}	4.1×10^{-3}	9.2×10^{-3}	1.2×10^{-1}
36XS	2.4×10^{-3}	5.1×10^{-3}	7.5×10^{-3}	1.2×10^{-1}
2535Nb	2.3×10^{-4}	7.0×10^{-3}	1.1×10^{-2}	1.2×10^{-1}
800H	1.3×10^{-4}	4.6×10^{-3}	1.4×10^{-2}	7.9×10^{-2}
HK40	4.3×10^{-3}	5.1×10^{-3}	1.3×10^{-2}	8.7×10^{-2}

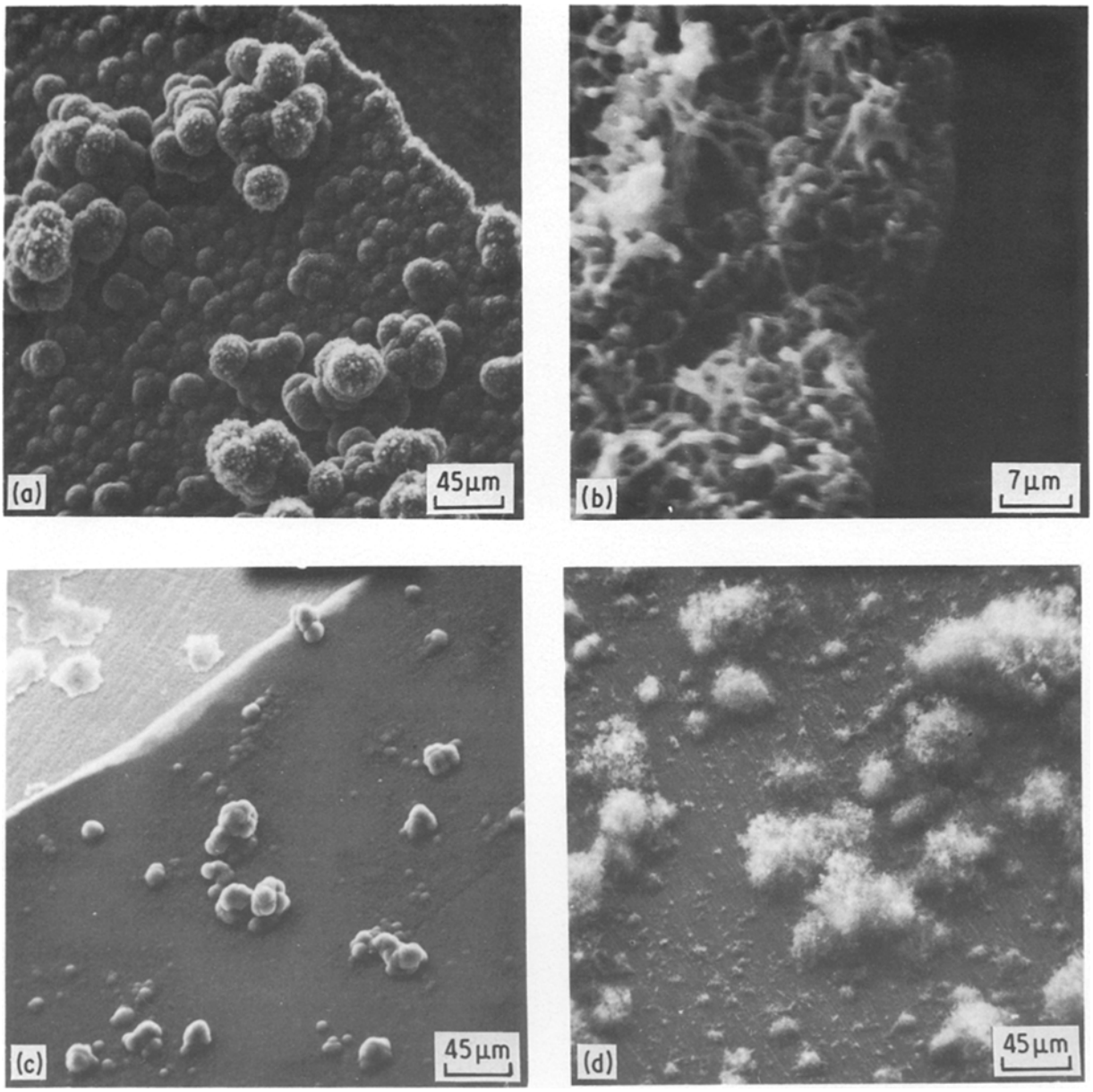

Figure 5 Scanning electron micrographs of surfaces of nickel and HK40 specimens coked in 3:1 hydrogen–propylene atmospheres. (a) Nickel, 1000° C; (b) nickel, 900° C; (c) HK40, 1000° C; (d) HK40, 600° C.

across the particle, including temperature gradients arising from exothermic decomposition of the gas and concentration gradients arising from supersaturation of the particle at the gas interface due to carbon activities greater than 1 in the gas phase [16]. A chemical potential gradient of dissolved carbon could also arise within the metal particle due to its small radius of curvature [17]. Since filamentous coke can form from gases which decompose endothermically, it is more probable that such a gradient provides the driving force for catalytic coke formation.

In the intermediate temperature region between 550 and 900° C, where the steady state coking rate of nickel decreased with increasing temperature, the observed negative activation energy may be attributed to adsorption effects [16] resulting in a reduction of the catalytic surface area with increasing temperature.

Above 900° C a positive activation energy was observed and is consistent with the gas-phase formation of pyrolytic carbon being the rate-controlling step.

Between 700 and 1000° C a similar activation energy was found for copper. As no filamentous coke was formed, copper is considered to be non-catalytic and the kinetics may be attributed solely to homogeneous gas-phase reactions. Within the limits of experimental reproducibility, identical steady state coking rates were observed for all materials between 900 and 1000° C, indicating coke formation was due essentially to gas-phase pyrolysis. Catalytic coke

TABLE IV Parabolic rate constants ($mg^2 cm^{-4} min^{-1}$) in 50:1 hydrogen–propylene atmospheres at 900° C

Material	36XT	36XS	2535Nb	800H	HK40	Ni
k_p	5.3×10^{-3}	1.2×10^{-2}	9.4×10^{-3}	7.7×10^{-3}	4.8×10^{-2}	5.6×10^{-3}

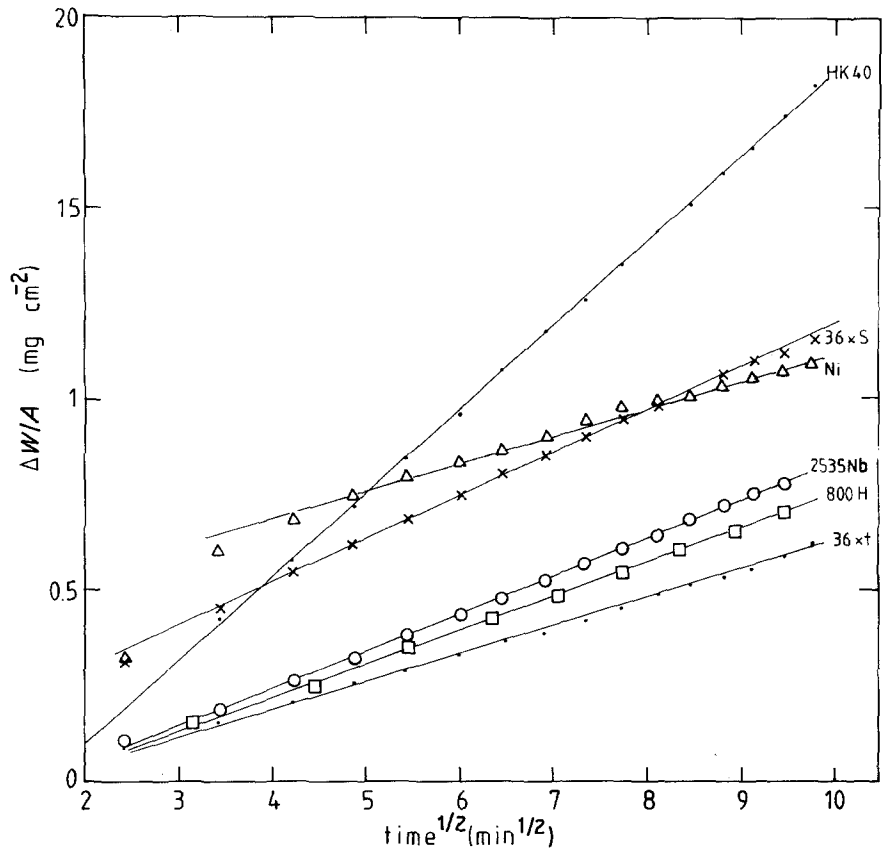

Figure 6 Parabolic plot of reaction kinetics at 900° C in 50:1 hydrogen–propylene atmospheres.

formation was considered to be of little importance at these high temperatures and even though some coke filaments were formed at 900° C the bulk of the coke deposit was pyrolytic.

Below 900° C catalytic coke formed only at localized sites on the surfaces of the alloys and only minor variations in coking rates and coke morphologies were observed at 800° C. Between 700 and 900° C it is considered that pyrolytic and catalytic coke formation contributed to the overall weight uptake of the specimens because all surfaces of the reactor were covered in pyrolytic coke.

At 700° C similar coke morphologies were observed; however, the large variation in steady state coking rates of the alloys appeared to result from variations in the quantity of filamentous coke formed on each Under these reaction conditions, the alloy surfaces formed chromium carbide scales. The absence of coke from all areas except localized sites indicates the non-catalytic nature of chromium carbide scales to coke formation. Coke morphologies formed below 900° C are consistent with a model proposed previously [15], where catalytic coke forms at failure sites in the chromium carbide scales. At such sites, a chromium-depleted iron–nickel alloy is exposed, catalytic metal particles are removed from the matrix and filamentous coke forms. The resulting coke morphologies observed on all materials in 3:1 hydrogen–propylene atmospheres are represented schematically in Fig. 11.

4.2. Coke formation at hydrogen–propylene ratios greater than 3:1

An attempt was made to induce the formation of catalytic coke on the alloys at 900° C, a temperature appropriate to the steam cracking of olefins to produce ethylene. Surface examination of nickel specimens coked at this temperature in atmospheres of varying hydrogen : propylene ratios, indicated that the proportion of filamentous to pyrolytic coke increased at the higher gas ratios. Consequently, subsequent alloy coking experiments were performed at 900° C in 50:1 hydrogen–propylene atmospheres and the resulting coke morphologies are shown schematically in Fig. 11.

Weight gain kinetics at 800° C for nickel and at 900° C for both nickel and the alloys differed greatly from those observed at all other temperatures. Parabolic kinetics were observed for the alloys in 50:1 hydrogen–propylene atmospheres for the entire duration of an experiment and in 3:1 hydrogen–

TABLE V X-ray diffraction analyses of surfaces of alloys coked in 3:1 and 50:1 hydrogen–propylene atmospheres at 900° C

Alloy	700° C	800° C	900° C	1000° C
Copper	graphite	–	graphite	graphite
Nickel	–	–	graphite	–
36XT	–	Cr_3C_2	Cr_3C_2	graphite, Cr_3C_2, Cr_7C_3
36XS	Cr_3C_2, Cr_7C_3	Cr_3C_2, Cr_7C_3	Cr_3C_2, Cr_7C_3	Cr_3C_2, Cr_7C_3
2435Nb	Cr_3C_2, Cr_7C_3	Cr_3C_2, Cr_7C_3	Cr_7C_3	graphite, Cr_7C_3
800H	Cr_7C_3	Cr_7C_3	graphite, Cr_7C_3	graphite, Cr_7C_3
HK40	Cr_7C_3	Cr_7C_3	graphite, Cr_7C_3	–

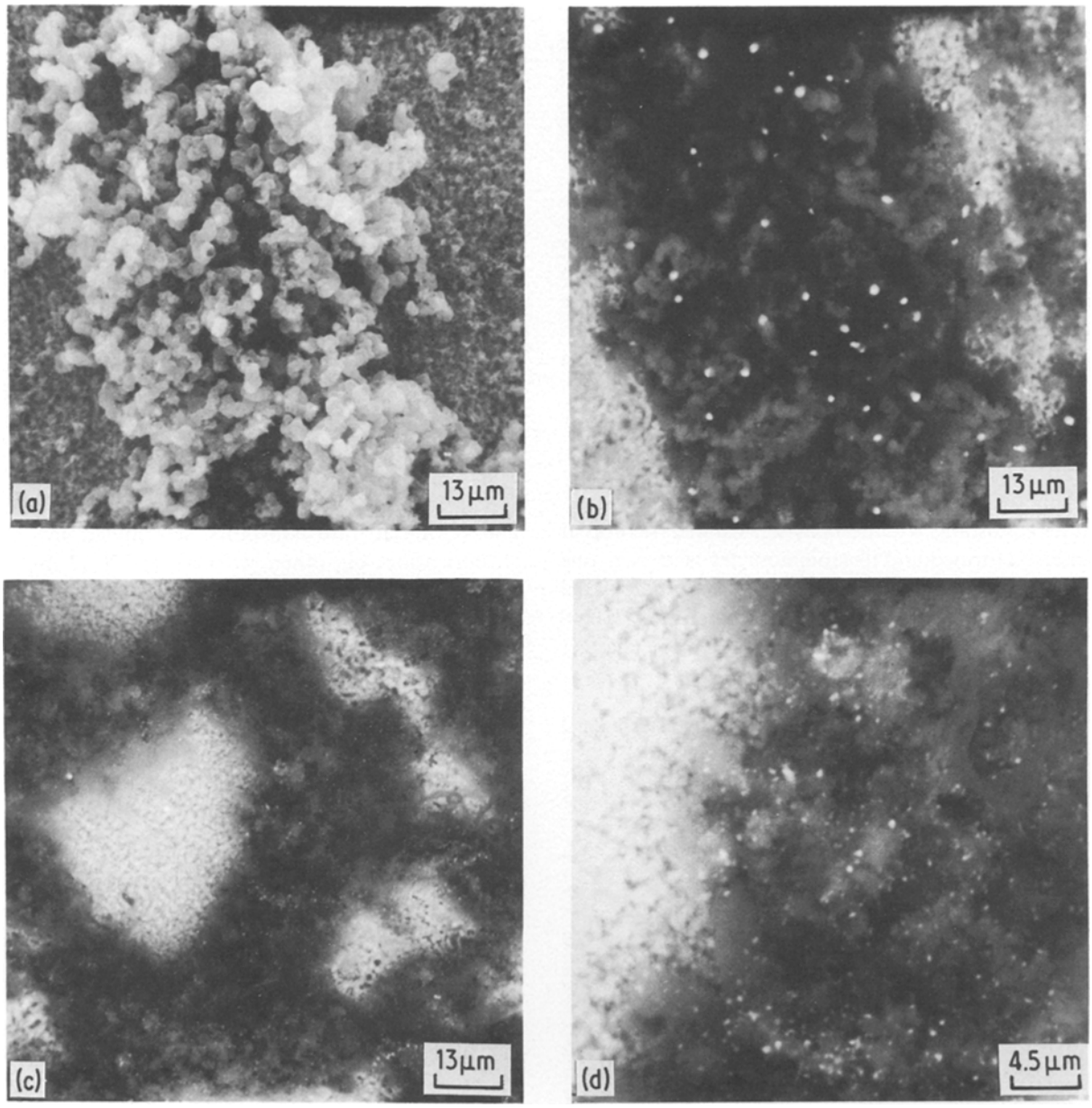

Figure 7 Scanning electron and backscattered electron (BSE) micrographs of surface of nickel and HK40 specimens coked in 50:1 hydrogen–propylene atmospheres at 900° C.

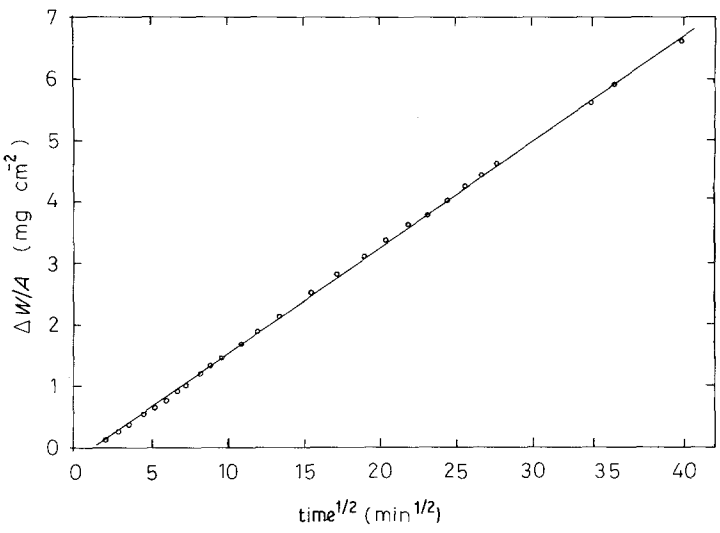

Figure 8 Coking kinetics of HK40 in 50:1 hydrogen–propylene at 900° C.

propylene atmospheres for periods of at least 1 h. When either catalytic or pyrolytic coke formation are rate-controlling reactions, linear kinetics may be expected; however, if the rate of carbon uptake is controlled by carbon diffusion into the metal, then very different kinetics result, as will be discussed.

4.3. Combined coking and carburization

It is generally considered that Wagner's model for internal oxidation of alloys [18] may be applied to carburization kinetics [1, 6]. In these models, it is assumed that inward diffusing carbon reacts with essentially all the free alloy chromium to form chromium carbide precipitates. The carbide reaction front advances into the alloy, at a rate controlled by inward carbon diffusion and parabolic kinetics results. Parabolic rate constants can be determined either gravimetrically or from carbide depth measurements. Under conditions where a constant volume fraction of carbide is formed and its stoichiometry is known, one type of parabolic rate constant can be easily calculated from the other. It has been shown for the alloy HK40 [2], however, that the carbide volume fraction changes considerably as a function of distance into the alloy and as a function of time, for a given temperature. For this reason, only gravimetric rate constants can be used for comparison with the presently reported kinetic behaviour.

TABLE VI Parabolic rate constants ($mg^2 cm^{-4} min^{-1}$) for carburization in hydrogen–methane atmospheres

Alloy	Composition	k_p
Schnaas and Grabke [1] 900° C, hydrogen–methane, $a_c = 1$		
800, 802	Fe–33Ni–21Cr–0.3Si	1.5×10^{-2}
61–16	Fe–61Ni–16Cr–3.3Si	1.7×10^{-3}
Norton *et al.* [5] 925° C, hydrogen–methane, $a_c = 0.8$		
HK30	Fe–21Ni–25Cr–0.3C–1.4Si	1.0×10^{-2}
314	Fe–20Ni–24Cr–2Si	7.2×10^{-3}
25Cr–20Ni	Fe–20Ni–24Cr	1.8×10^{-2}

The general similarities between present results and parabolic rate constants determined for alloy carburization by other workers [1–5] (Table V), strongly supports the view that weight uptake kinetics at 900° C in 50:1 hydrogen–propylene atmospheres result from alloy carburization. In addition, the final carbon uptake of a specimen of HK40 (approximately 0.1 cm^3) almost completely carburized after 4 days, (Fig. 10) was 16 mg. As very little coke was present on the alloy surface after this time (Fig. 10a), it may be assumed that all the deposited carbon reacted to form chromium carbides. Metallographic examination of the specimen cross-section and XRD revealed that only Cr_7C_3 was formed. On this basis, the free chromium concentration in the original alloy was calculated to be 20 wt %, in agreement with the actual value for HK40.

In the case of nickel, which does not form any stable carbides at 900° C, the dissolved carbon concentration can be approximated from the solution of Fick's second law for an infinite system having a constant surface concentration of the diffusing component [19]. The result is:

$$C(x, t) = C''\left[1 - \operatorname{erf}\left(\frac{x}{2D^{1/2}t^{1/2}}\right)\right]$$

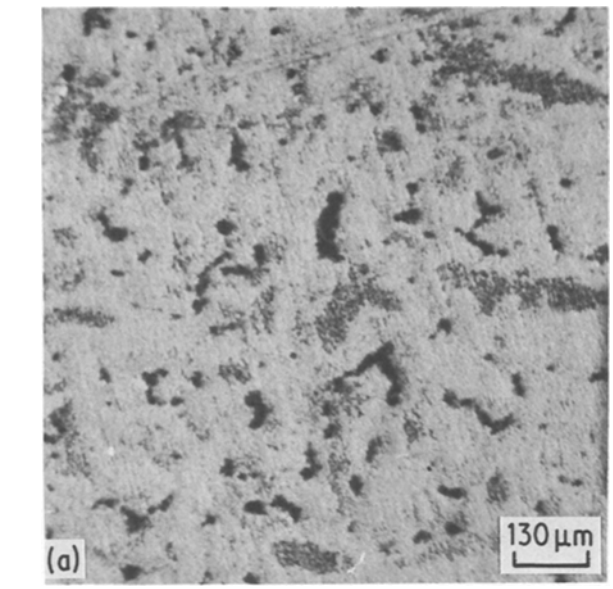

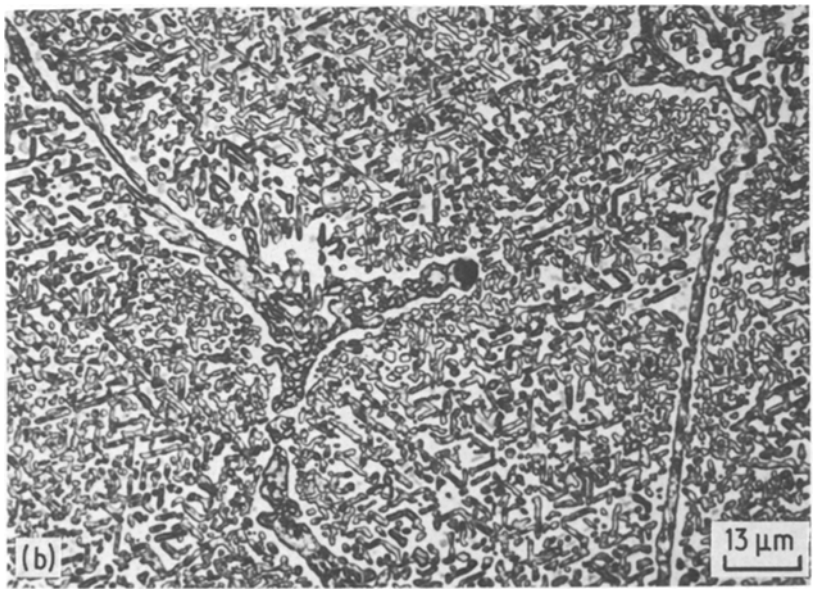

Figure 9 Surface morphology (a) and etched cross-section (b) of HK40 coked for 4 days at 900° C in 50:1 hydrogen–propylene.

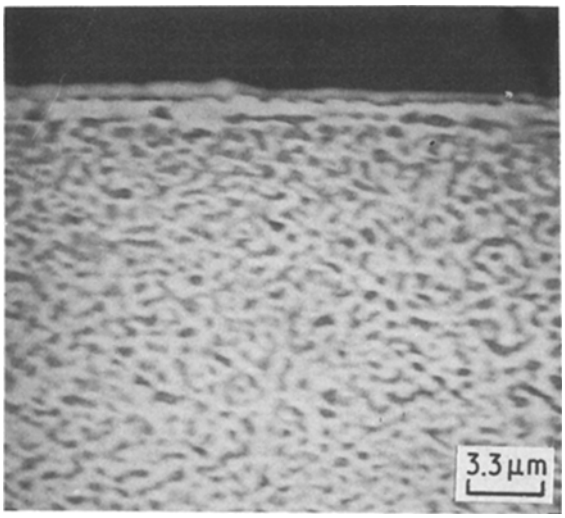

Figure 10 Scanning electron micrograph of typical thin chromium carbide scale formed at 900 to 1000° C.

where $C(x, t)$ denotes concentration at time, t and distance, x from the surface; C'' is the surface concentration, given by the solubility of carbon in nickel, D is the diffusion coefficient and erf, the error function. The total carbon uptake, ΔW, is obtained by integrating the above expression [20] between $x = 0$ and $x = \infty$ which yields:

$$\Delta W/A = 1.1284\, C''(Dt)^{1/2}$$

Substitution of values for carbon solubility in nickel [21] ($0.0178\,g\,cm^{-3}$) and the diffusion coefficient [22] ($5.55 \times 10^{-9}\,cm^2\,sec^{-1}$) into the above equation, yields a value of $1.34 \times 10^{-4}\,mg^2\,cm^{-4}\,min^{-1}$ for the parabolic rate constant for carbon diffusion in nickel. The lack of agreement between this and the value determined experimentally from Fig. 4 ($5.6 \times 10^{-3}\,mg^2\,cm^{-4}\,min^{-1}$) shows that the kinetics observed for nickel cannot be ascribed to carbon diffusion into the metal.

Parabolic rate constants for weight uptakes in 3:1 hydrogen–propylene atmospheres were generally almost double those in 50:1 atmospheres indicating that processes other than carburization, which is temperature dependent only, contributed to the total specimen weight. Coke morphologies in this atmosphere consisted of an external compact coke layer containing some filamentous coke above a severely carburized alloy, indicating the importance of coke formation as well as carburization on the overall weight uptake kinetics. It is likely that the parabolic behaviour observed in 3:1 atmospheres may arise from a steady decrease in catalytic surface area as time proceeds, due to partial poisoning of the catalyst particles by the deposition of carbon as has been observed frequently for nickel in other hydrocarbon gases [16, 23, 24].

The differences in parabolic rate constants of nickel and the alloys in 50:1 and 3:1 gas mixtures can be explained in terms of the two processes described above. Thus the richer hydrocarbon atmosphere gives rise to coking as well as carburization, producing a higher value of k_p in the initial stage of reaction. Subsequently, a steady state coking process occurs at a rate far in excess of the carburization process and overall linear kinetics result.

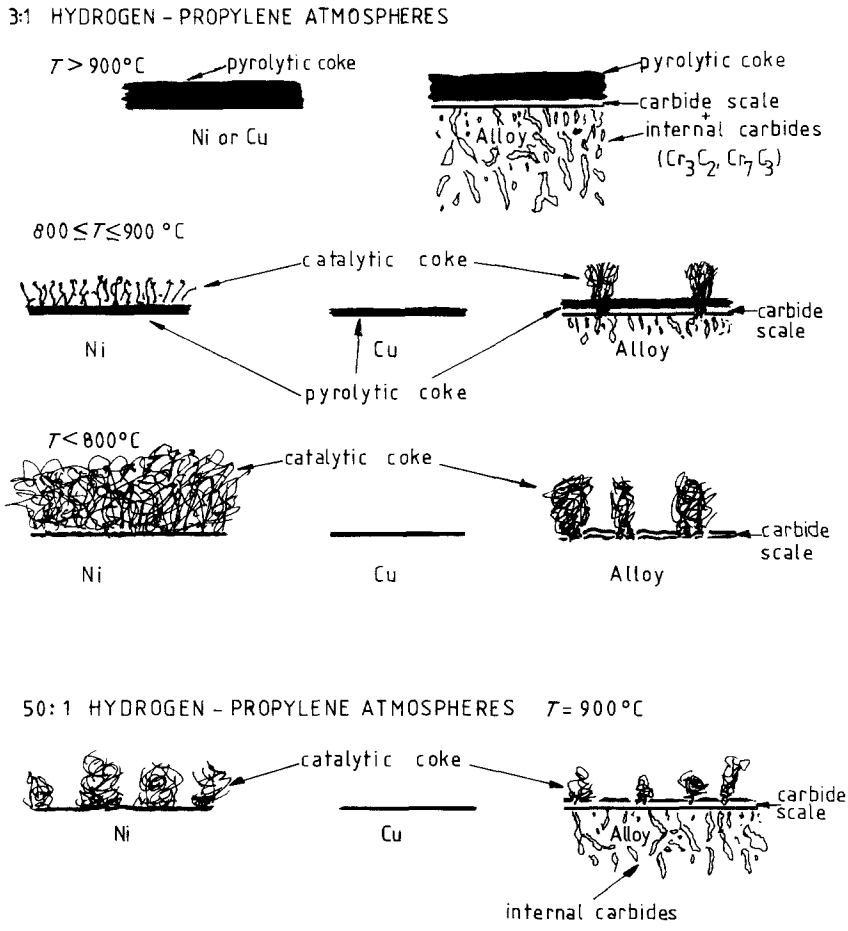

Figure 11 Schematic representation of coke morphologies observed in hydrogen–propylene atmospheres.

5. Conclusion

The rate of coke formation on alloys increased continuously between 500 and 1000° C. Between 900 and 1000° C steady state kinetics were controlled by gas-phase pyrolysis and similar reaction rates were observed for all materials. Alloy carburization and catalyst poisoning effects at 900° C resulted in initial periods of non-linear kinetics, with durations which increased with the ratio of hydrogen to propylene in the atmosphere. Below 900° C it appeared that catalytic coking on alloys occurs where local failure sites in the chromium carbide scales expose a chromium-depleted substrate to the gas atmosphere. Differing catalytic activities resulted in significant differences in coking rates between nickel and copper below 900° C, whereas significant differences in reaction rates of alloys due to formation of filamentous coke were observed only below 800° C. These differences arose from variation in the effectiveness of the carbide scales in excluding the gas from contact with the underlying nickel- and iron-rich alloy.

References

1. A. SCHNAAS and H. J. GRABKE, *Oxid. Met.* **12** (1978) 387.
2. J. M. HARRISON, J. F. NORTON, R. T. DERRICOTT and J. B. MARRIOTT, *Werkst. Korros.* **30** (1979) 785.
3. T. A. RAMANARAYANAN and R. PETKOVIC-LUTON, *Corrosion* **37** (1981) 712.
4. R. H. KANE, *ibid.* **37** (1981) 187.
5. J. F. NORTON, L. BLIDEGN, S. CANETOLI and P. D. FRAMPTON, *Werkst. Korros.* **32** (1981) 467.
6. G. M. SMITH, D. J. YOUNG and D. L. TRIMM, *Oxid. Met.* **18** (1982) 229.
7. D. J. HALL, M. K. HOSSAIN and R. F. ATKINSON, *High Temp. High Press.* **14** (1982) 527.
8. P. TOMAS, D. J. YOUNG and D. L. TRIMM, Proceedings of the 9th International Congress on Metallic Corrosion, Toronto, Canada, 3–7 June 1984, Vol. 1 (National Research Council of Canada, Ottawa, 1984) p. 58.
9. J. C. MAREK and L. F. ALBRIGHT, in "Coke Formation on Metal Surfaces", edited by L. F. Albright and R. T. K. Baker, ACS Symposium Series, (American Chemical Society, New York, 1981) pp. 123, 151.
10. D. E. BROWN, J. T. K. CLARK, A. I. FOSTER, J. J. McCARROLL and M. L. SIMS, *ibid.*, p. 23.
11. D. L. TRIMM, *Catal. Rev. Sci. Eng.* **16** (1977) 155.
12. *Idem*, in "Pyrolysis: Theory and Industrial Practice", edited by L. F. Albright, B. L. Crynes and W. H. Corcoran (Academic Press, New York, 1983) p. 203.
13. M. J. BENNETT and J. B. PRICE, *J. Mater. Sci.* **16** (1981) 170.
14. A. I. LACAVA, E. D. FERNADEZ-RAONE and M. CARABALLO, in "Coke Formation on Metal Surfaces", edited by L. F. Albright and R. T. K. Baker, ACS Symposium Series, (American Chemical Society, New York, 1981).
15. P. TOMASZEWICZ, P. R. S. JACKSON, D. L. TRIMM and D. J. YOUNG, *J. Mater. Sci.* **20** (1985) 4035.
16. J. ROSTRUP-NIELSEN and D. L. TRIMM, *J. Catal.* **48** (1977) 155.
17. R. E. SMALLMAN, "Modern Physical Metallurgy", 3rd Edn (Butterworth, London, 1976).
18. R. A. RAPP, *Corrosion* **21** (1965) 382.
19. P. G. SHEWMON, "Diffusion in Solids", (McGraw-Hill, New York, 1963).
20. H. S. CARSLAW and J. C. JAEGER, "Conduction of Heat in Solids", 2nd Edn (Clarendon Press, Oxford, 1959).
21. T. WADA, H. WADA, J. F. ELLIOTT and J. CHIPMAN, *Met. Trans.* **2** (1971) 2199.
22. I. I. KOVENSKIY, *Phys. Met. Metallogr.* **16** (1963) 107.
23. Y. NISHIYAMA and Y. TAMAI, *J. Catal.* **30** (1973) 86.
24. C. BERNARDO and L. S. LOBO, *ibid.* **37** (1975) 267.

Received 7 August
and accepted 23 October 1985